ASSESSMENT OF RADIATIVE HEAT TRANSFER IMAPCT ON A TEMPERATURE DISTRIBUTION INSIDE A REAL INDUSTRIAL SWIRLED FURNACE

*Filip JURIĆ[1], Milan VUJANOVIĆ[*1], Marija ŽIVIĆ[2], Mario HOLIK[2], Xuebin WANG[3], Neven DUIĆ[1]*

[1]Faculty of Mechanical Engineering and Naval Architecture, University of Zagreb, Ivana Lučića 5, 10000 Zagreb, Croatia

[2]Mechanical Engineering Faculty, Josip Juraj Strossmayer University of Osijek, Trg Ivane Brlić Mažuranić 2, Slavonski Brod, Croatia

[3]MOE Key Laboratory of Thermo-Fluid Science and Engineering, Xi'an Jiaotong University, Xi'an, Shaanxi 710049, China

[*]Corresponding author; E-mail: milan.vujanovic@fsb.hr

Combustion systems will continue to share a portion in energy sectors along the current energy transition, and therefore the attention is still given to the further improvements of their energy efficiency. Modern research and development processes of combustion systems are improbable without the usage of predictive numerical tools such as Computational Fluid Dynamics (CFD). The radiative heat transfer in participating media is modelled in this work with Discrete Transfer Radiative Method (DTRM) and Discrete Ordinates Method (DOM) by finite volume discretisation, in order to predict heat transfer inside combustion chamber accurately. DTRM trace the rays in different directions from each face of the generated mesh. At the same time, DOM is described with the angle discretisation, where for each spatial angle the radiative transport equation needs to be solved. In combination with the steady combustion model in AVL FIRE™ CFD code, both models are applied for computation of temperature distribution in a real oil-fired industrial furnace for which the experimental results are available. For calculation of the absorption coefficient in both models weighted sum of grey gasses model is used. The focus of this work is to estimate radiative heat transfer with DTRM and DOM models and to validate obtained results against experimental data and calculations without radiative heat transfer, where approximately 25 % higher temperatures are achieved. The validation results showed good agreement with the experimental data with a better prediction of the DOM model in the temperature trend near the furnace outlet. Both radiation modelling approaches show capability for the computation of radiative heat transfer in participating media on a complex validation case of the combustion process in oil-fired furnace.

Key words*: Radiative Heat Transfer, Participating Media, Furnace, Radiative Absorption, Combustion*

1. Introduction

It is known that the radiative heat transfer as a fundamental heat transfer mechanism is not negligible in the overall heat transfer of the energy systems that work at the high-temperature conditions. Recent researches show that if emissions concentrations are to be calculated, it is not enough to exclude the impact of radiation on overall heat transfer and consequently, on emission formation [1]. In numerical modelling of engineering systems that operate at high temperatures such as furnaces, boilers, jet engines and internal combustion engines the consideration of radiative heat transfer in calculations significantly influence the energy efficiency [2]. As one of the predictive tools in energy efficiency investigation, the Computational Fluid Dynamics (CFD) is frequently utilised for the research of combustion system designs to evaluate the heat transfer impact on their energy efficiency [3]. With the development of the computational resources, the radiative heat transfer models within CFD are commonly applied to evaluate the impact of the radiative heat transfer impact on total heat transfer and temperature distribution [4]. For the calculation of radiative heat transfer in participating media of furnace combustion chamber, in this work, two radiation models have been applied: Discrete Transfer Radiation Method (DTRM) and Discrete Ordinates Method (DOM) approximation with a finite volume approach. Both models are employed within the CFD software AVL FIRE™. These two models have different modelling approach in solving the radiative transfer equation of participating media by their definition [5]. The DTRM model is based on the raytracing, which calculates the radiation intensity through the computational domain and has an utterly different modelling procedure from DOM featuring finite volume method [6]. In the pre-processing stage, the raytracing procedure is executed for each ray that is shot from the boundary face. The path through the computational domain is being calculated [7]. The input data of DTRM is a number of rays shot from the face, where for a greater number of rays, the more precise results will be obtained but will require more computational time [8]. For the DOM model, the input number of azimuthal and polar angles needs to be defined. After the spatial discretisation is conducted, the radiative heat transfer equation is calculated with transport equations for incident radiation in each spatial angle that represents one ordinate. Contributions of each ordinate are summed and added as input for calculation of the radiative source term in the energy conservation equation [9]. The authors of [10] show universality of DOM to be applied to a whole range of applications. The algorithm for obtaining ordinates directions and their spatial angles is described in [11]. Both modelling approaches (DTRM and DOM) are equally computationally demanding, and their accuracy is adjustable with input parameters [12]. Additionally, in this work, the absorptivity and emissivity are modelled as for isotropic media while the scattering phenomenon was not considered in observed simulations, since the soot participation in radiative heat transfer is well described by the grey-body model [13].

The recent research for optimising the combustion process by using CFD in combustion chambers showed that the application of radiative properties of the gas inside the steady system such as jet engine combustion chamber cannot be neglected [14]. The similar approach for investigating radiative heat transfer impact was used in the numerical modelling of heat transfer in strong swirl flow of furnaces [15]. In [16], the authors performed analysis of thermal efficiency with emphasis on the radiative impact calculated by DOM in reheating furnace. AVL FIRE™ was already employed for steady calculations in biomass combustion in a rotary kiln in [17], where the similar framework is applied for the simulations in this work.

For the assessment of radiative heat transfer impact on temperature distribution in this work, IJmuiden furnace is selected for which dimensions and experimental data is available in [18]. The combustion process is modelled with Steady Combustion Model (SCM) based on literature [19], where it was applied with and without heat transport by radiation. This SCM features fast convergence and steady solution of the combustion process and is applicable for the combustion process in oil-fired utility [20]. It is computationally less demanding compared to the extended combustion models generally utilised in combustion systems like in [21]. A similar approach was applied for experimental oil furnace for emission predictions, but without radiation [22]. For the boundary conditions, diffusive opaque and inlet/outlet boundary conditions were applied for the calculation of incident radiation in directions that are oriented into the computational domain, based on the [23]. Similar approach was employed in [24], where the furnace gas temperature is predicted in reheating furnace with the P-1 radiation model. In [25], the estimation of radiative heat transfer in pulverised coal combustion is performed with the P-1, where the impact of particulate impact on incident radiation scattering is assumed.

Finally, this work aims to present the analysis of the radiative heat transfer in participating media with two different radiation models, DTRM and DOM in combination with Steady Combustion Model by employing CFD code AVL FIRE™ on an industrial furnace which includes the swirled combustion process. The performed validation of both radiative heat transfer models has shown that the presented modelling procedures are capable of predicting heat transport and can be used as a computationally fast tool that facilitates design and optimisation of industrial furnaces. The results with DTRM and DOM showed agreement in the validation against the experimental results. The results with DTRM and DOM showed agreement in the validation against the experimental results. All numerical simulations are performed with 20 CPU Intel® Xeon® E5-2650 v4 @ 2.20 GHz.

2. Mathematical model

All simulations performed in this paper are described with Reynolds-Averaged Navier-Stokes equations. The Reynolds stress tensor was modelled by using the $k - \varepsilon$ turbulence model, which details can be found in [26].

2.1. Combustion modelling

The combustion process was modelled by SCM, which calculates a fast solution for the combustion process in oil-fired furnaces [20]. SCM is based on empirical correlations for considering the impact of droplet evaporation, swirl motion, spray disintegration, chemistry kinetics on the oil combustion in an extended Arrhenius type expression. Additionally, SCM is applicable for the wide range of conventional oil flames. In SCM, the oil fuel is assumed in pre-mixed regime with the primary air flow, due to consideration of the mixing time in combustion velocity. The model considers different reaction rate calculation:

$$\bar{r} = -\rho \frac{\upsilon\, y_{fu}}{\partial t} = -k\, \rho\, \overline{y_{fu}}\, \overline{y_{O_2}} \tag{1}$$

where k is the reaction rate constant, $\overline{y_{fu}}$ the average fuel mass fraction and $\overline{y_{O_2}}$ the average oxygen mass fraction, which is considered in the Equation (1) if $\overline{y_{O_2}}$ is lower than 0.03. Constant k could be characterized as a combustion velocity and is obtained from the following equation:

$$k = \frac{\upsilon}{t_{} + t_{} + t_{}} \tag{2}$$

where the combustion velocity coefficient b is considered 33 for the $\overline{y_{O_2}}$ lower than 0.03 and 1 for $\overline{y_{O_2}}$ higher than 0.03, due to the influence of sufficient oxygen. The denominator of the Equation (2) is called total time, and it consists of three elements:

Time of evaporation and induction, t_{ei}

$$t_{ei} = A \, e^{\frac{10}{RT}} + 0.45695 \, d_{init}^{\;2} \tag{3}$$

with T as local temperature, R as the universal gas constant and d_{init} as initial droplet diameter of value 0.3 mm. Time of oxidation, t_{ox}

$$t_{ox} = \frac{u_{init}}{0.0023 \, (T \quad 273.15) \quad 1.79} \tag{4}$$

In SCM fluid flow is calculated only for one gaseous phase, which results that the evaporation process of inlet fuel is modelled inside the evaporation and induction time in Equation (3). Further description about evaporation time calculation can be found in literature [27]. This model gives good coverage of kinetic combustion for the lean region and for the burning of evaporated fuel in the region of disintegrated droplets. In SCM, the values b is adjusted for different values when oxygen concentrations, which makes the reaction rate dependent on the availability of oxygen [20]. The mixing process of air and evaporated fuel in this work is amplified by the swirl motion of the primary inlet air. The inlet swirl velocity of primary air is defined by user-functions in the AVL FITE™, where the swirl ratio of 0.8 value around the x-axis is used. Additionally, this model is also suitable for calculating the flames formed in furnaces with the additional secondary inlet of air.

2.2. Radiative Heat Transfer Modelling

In this subsection, two different modelling approaches that are used in this paper for the calculation of radiative heat transfer are presented: DTRM and DOM.

2.2.1   Discrete Transfer Radiative Method (DTRM)

The primary assumption of the DTRM is that a single ray can approximate the radiation leaving the surface element in a specific range of solid angles. Such an assumption of DTRM is made by employing raytracing, where the change of incident radiation of each ray is only followed until the ray hit the wall [28]. The shift in incident radiation along a ray path can be written as:

$$\frac{dI}{ds} = \frac{a\sigma T^{}}{\pi} - aI \tag{5}$$

where a change of incident radiation is equivalent to a difference of the emitted and absorbed incident radiation. For this research, the refractive index is assumed 1. The DTRM integrates Equation (5) along with a series of rays leaving the boundary faces. The incident radiation is defined as $I(s)$ is calculated as [29]:

$$I(s) = \frac{\sigma T^{\cdot}}{\pi}(1 - e^{-as}) + I_0 e^{-as} \qquad (6)$$

In the pre-processing, the raytracing paths are computed and saved before the start of fluid flow calculations. An azimuthal angle from which the rays are shot is varied from 0 to $\pi/2$ and polar from 0 to 2π. For each ray, length within each control volume that it intercepts is calculated and stored. All wall boundaries are taken as black and diffuse. Thus, the intensity leaving the wall is given as:

$$I_{bnd} = \frac{\sigma T_w^{\cdot}}{\pi} \qquad (7)$$

where T_w is the wall temperature and σ is Stefan-Boltzmann constant. That means that the outgoing radiation flux is composed only of the directly emitting. The incident radiation at inlets and outlets leaves the calculation domain. Therefore, it is not reflected on inlet and outlet boundaries, and it is calculated as:

$$I_{bnd} = \frac{\sigma T_{of}^{\cdot}}{\pi} \qquad (8)$$

where T_{of} is the temperature of the outflow boundary. The incident radiation flux at the boundary element is then calculated as the sum of incident intensities for all rays. In participating media, the energy gain or loss in internal cells due to radiation is given through the radiation source term. The radiation source term is then inserted as source term of the enthalpy conversation equation. The overall energy gain or loss for a specific internal cell is calculated from the sum of all rays the contributions crossing the cell.

2.2.2 Discrete Ordinates Method (DOM)

The radiation in participating media was also modelled by the DOM model featuring a finite volume approach. The radiative heat transfer in the DOM is based on solving Radiative Transfer Equation (RTE), which is consisting of two mechanisms: absorption and emission. Participating media absorbs the incoming radiation, which is then enhanced by the emission of the media in different directions.

$$\frac{\sigma T^{\cdot}}{\partial s^l} = -(a + \sigma_s)I^l + a\left(\frac{\sigma T^{\cdot}}{\pi}\right) \qquad (9)$$

The I^l in the Equation (9) is the intensity of incident radiation in the l direction, a is the absorption coefficient, and s^l is an ordinate direction with its spatial angle $\Delta\Omega^l$. Spatial angle discretization is defined as the ordinate direction s^l is oriented perpendicular to its spatial angle. Equation (9) has to be solved for each discretised spatial angle, but the minimal number is recommended to be eight [13]. When the intensity of incident radiation in each ordinate direction is obtained, the incident radiation is calculated as:

$$G = \sum I^l \cdot \Delta\Omega^l \qquad (10)$$

where n is the total number of control angles that is defined by discretisation of spatial angles. It can be noticed from Equation (10) that the incident radiation depends mainly on the temperature, where the interaction between the radiation heat transfer and the radiative power source is modelled as in Equation (11).

$$S_{rad} = a(G - 4\sigma T^4) \tag{11}$$

The boundary conditions in this work are assumed as the diffusive walls and are calculated only for the ordinates that have an orientation in the computational mesh. Diffusive opaque walls are defined as [10]:

$$I_{bnd}^l = \epsilon \frac{n_r \sigma I}{} + (1 - \epsilon) \frac{\angle(s^l \cdot n_i) > 0}{} \frac{I^l D_{ci}}{D} \tag{12}$$

where ϵ is the wall emissivity, and D_{ci} are auxiliary variables for solving orientations of spatial angles in regards to cell face orientation. For the calculation intensities of incident radiation in Equation (9), the upwind differencing scheme is applied. Convergence criterium is defined as the ratio of the difference between the new and old value of incident radiation divided by the old incident radiation value, and in the following simulations equals 0.001.

2.3. Absorption coefficient modelling

Absorption coefficient in this work is modelled by implemented WSGGM for grey gases, which is based on the CO_2 and H_2O correlations in the literature [30]. The total absorption coefficient κ is defined as:

$$\kappa = -\frac{\ln(1 - \varepsilon)}{s} \tag{13}$$

Emissivity ε in Equation (13) is defined in Equation (14).

$$\varepsilon = \sum_{i=0}^{2} \alpha_i \left(1 - e^{-a_i p s}\right) \tag{14}$$

In Equation (14) α_i is weight factor of the grey gas i, a_i is its radiative absorption coefficient, p partial pressures of the of ith grey gas. The weighting factors of grey gas i are defined by the polynomial term for which the polynomial coefficient $b_{i,j}$ are tabulated.

$$\alpha_i = \sum_{j=0}^{3} b_{i,j} T^j \tag{15}$$

For i equals zero, the transparent gas is assumed. The weight factor of transparent gas is defined as:

$$\alpha_o = 1 - \sum_{i=0}^{2} \alpha_i \tag{16}$$

3. Numerical setup

In Figure 1, the computational mesh with around 177000 control volumes is generated, for which the mesh dependency test was performed on two finer meshes with the input cell size 66 % and 50 % of the initial cell size. Simulation performed on all three meshes showed flow, temperature and turbulence quantities with the relative deviation lower than 0.5 %. For the mass conservation equation, the Central Differencing Scheme (CDS) was employed. In contrast, for the turbulence, energy and volume fraction transport equations, the first order Upwind Differencing Scheme (UDS) was applied.

For the momentum equation, a combination of CDS and UDS was proposed by introducing a blending factor of 0.5. The convergence of the solution was achieved when the normalised pressure residual reached values lower than $5 \cdot 10^{-4}$ also, momentum and energy residuals lower than 10^{-4}. For turbulence, energy and volume fraction transport equations the first-order upwind differencing scheme was used, while for the continuity equation, the central differencing scheme was employed. For the momentum equation, the MINMOD Relaxed scheme was employed [20]. The convergence criteria were satisfied when normalised energy, momentum and pressure residuals reached a value lower than 10^{-4}. For the DOM the RTE was solved each twentieth fluid flow iterations. For the numerical simulations in this work crude oil fuel was modelled as a chemical compound with the average chemical formula $C_{13}H_{23}$, where the lower heating value is set to 41.1 MJkg^{-1}, and physical properties as density and viscosity are adopted from the AVL FIRE™ fuel database.
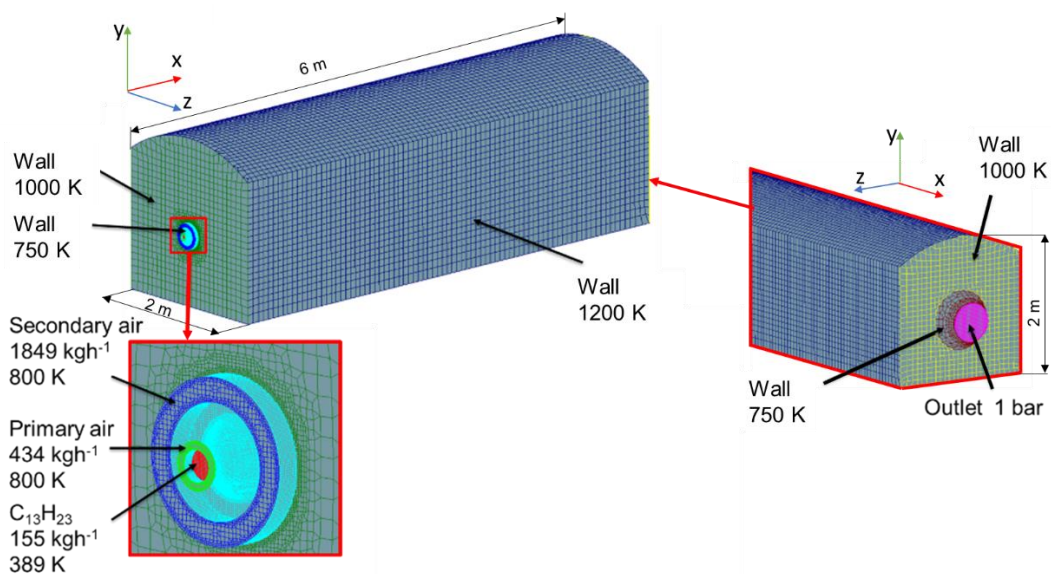

Figure 1   Computational domain with the boundary conditions

The boundary selections are shown in Figure 1, with the wall, inlet and outlet boundary conditions. The wall selections were defined as Dirichlet boundary condition of fixed temperature, and the air and fuel entrainment were prescribed with a constant temperature mass flow. In the following case, all wall boundaries are set with an emissivity value 1. At the outlet selection, the static pressure was prescribed. Characteristic for the IJmuiden furnace is the secondary air with four times larger mass flow. Spray parameters are considered inside the combustion model, which resulted in deficient computational time. That is precisely why this model is chosen for the combustion modelling in the furnace, to have an emphasis on the radiative heat transfer. For the DTRM raytracing, local hemisphere discretization was achieved with discretising boundary hemisphere with two polar angles and eight azimuthal angles. Thermal boundary under-relaxation factor was set to 0.5, and the tolerance was set to 0.01.

4. Results

In this section, critical specific objectives, the significant findings, and the most significant conclusions of the paper are presented. The presented temperature results for the verification furnace

case are calculated for the steady-state, where the convergence of results is achieved after approximately 3000 fluid flow iterations.

Figure 2 shows the results at the line connecting the centre of the inlet and centre of the outlet. The black dots represent experimental temperature measurements that are used for validation of radiation models. The blue curve shows results without radiation, that indicate overprediction of temperature results, and pronounced radiative gas emission losses in the furnace. The orange curve shows results obtained with the DTRM, while the green curve represents the results obtained with the DOM. The main difference between DTRM and DOM results is visible at the outlet of the domain, and it can be attributed to the outlet geometry that makes uncertainty raytracing. Furthermore, the better trend with calculation without radiation is achieved with the DTRM, which can be assign to lack of rays that hit the cells in the near outlet region.
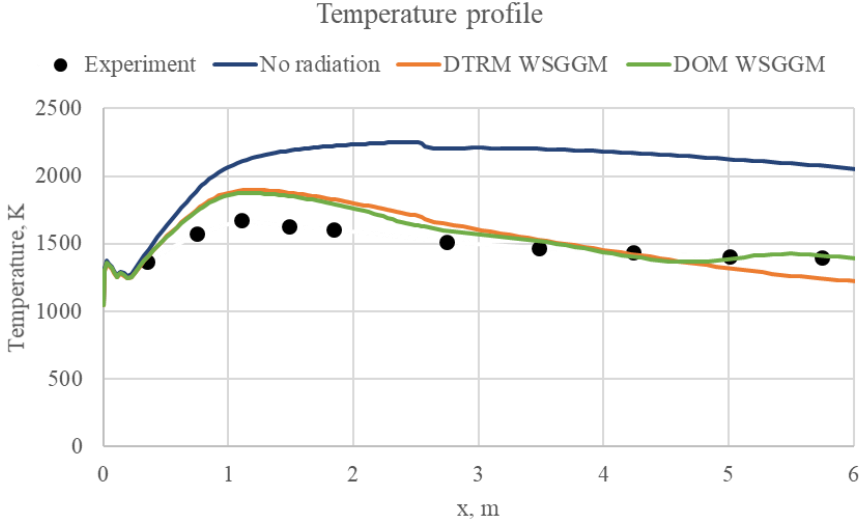

Figure 2   Temperature profile comparison between experimental data, combustion model without radiation and with DTRM and with DOM

Figure 3 shows measured distributions of unidirectional radiation intensity through a steady-state oil flame, where the results with radiation are showed against experimental results. Both models show good agreement with experimental results and with their trend. The DOM results have slightly overprediction compare to the DTRM results during the whole region, which is especially pronounced between 1.5 m and 2 m of flame. The difference in these results is the outcome from the model equations, that differently calculate the gas emission in the flame cells.
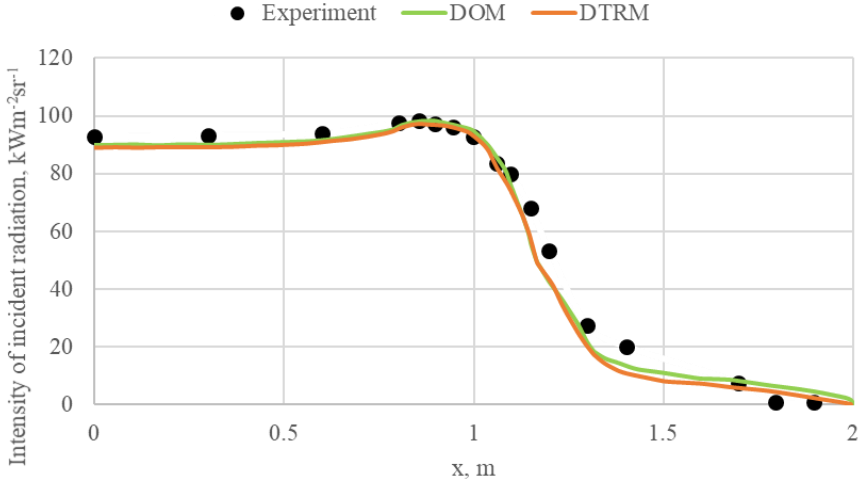
Figure 3 **Comparison between calculated and measured distributions of unidirectional radiation intensity through a steady-state oil flame**

In Figure 4, at the top, the temperature field results are shown for the case where the radiative heat transfer was not considered. The colder fuel region is visible near the inlet due to the lower air and fuel temperature. Inside the combustion chamber after the spray region, the practically uniform temperature field is achieved with the temperature of around 2200K.
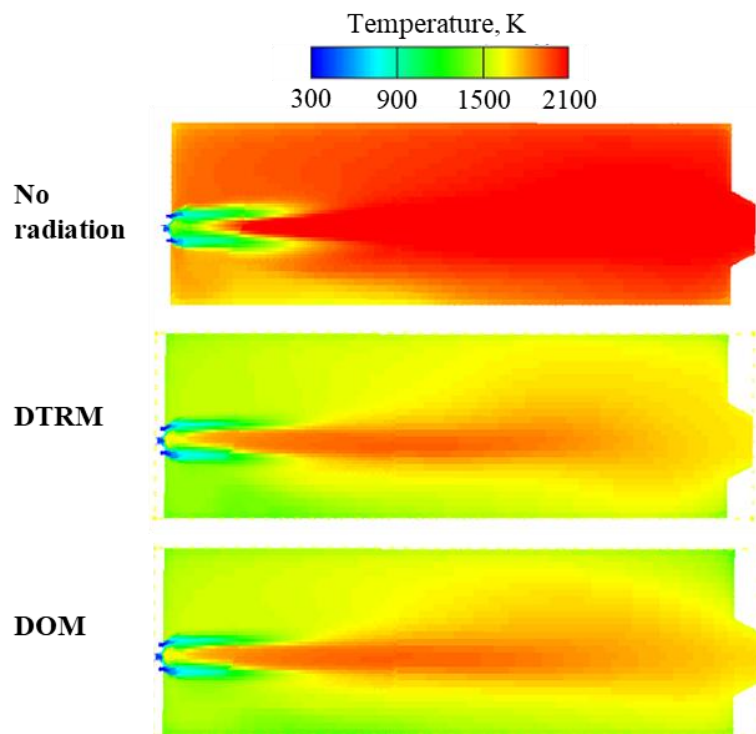

Figure 4 **Temperature field results at the symmetry plane of the computational domain**

DTRM and DOM results show a good agreement in a temperature distribution inside the combustion chamber. Difference between results with included radiative heat transfer and without radiation is in the near-wall temperatures and around the inlet, due to no presence of gas emissions in heat transfer. That can be attributed to the low-temperature region of the injected fuel and the high emissivity of the media near the walls. The lower mean temperature obtained in the simulations with included DTRM has a slightly broader and shorter flame region, which is especially visible in the area near the outlet, which is also evident in Figure 2 diagram. The computational time of the showed results is four times more expensive for DTRM case compared to the case without calculation of the radiative heat transfer in participating media. The DTRM pre-processing of raytracing contributes most to that difference, which needs to be calculated only once before the start of the first calculation. Additional computational demand of DTRM is also obtained due to low CPU parallelisation potential, where the communication between CPUs is aggravated by waiting for raytracing information, unlike the DOM where the parallelisation is faster.

5. Conclusion

The radiative heat transfer analysis in CFD of the steady combustion process provides a valuable tool that can be used to investigate more accurate and better understand the combustion process. The feasibility of DTRM and DOM radiative heat transfer models in the AVL FIRE™ code is examined, where the focus is on their comparison and application in combination with the combustion process inside a furnace combustion chamber. Simulations performed with steady combustion model are presented for three cases: without radiative heat transfer, with radiation calculated by DTRM and with radiation calculated by implemented DOM. The comparison of the computational time in the test cases showed that the calculations with DTRM is four times more expensive compared to the case without calculation of the radiative heat transfer in participating media, and DOM is around two times more expensive. The validation results showed good agreement with the experimental data with a better prediction of DOM model in the temperature trend near furnace outlet, which can be attributed to the shortcomings of DTRM raytracing in the near outlet region. The comparison of temperature distribution shows that the temperature field predicted with the DOM approach has a good agreement with the DTRM results, where a similar trend to the simulation without radiation is achieved. Furthermore, the main difference between DTRM and DOM results is visible at the outlet of the furnace, where the outlet geometry impacts the DTRM raytracing uncertainty. While for the DOM calculation, the incident radiation is calculated in every cell, which results in a better agreement with the experimental temperature profile along with the furnace. The calculations with the DTRM and DOM model are compared with the simulation without calculating radiative heat transfer, where approximately 25 % higher temperatures are reached. Finally, it can be stated that the presented method with DTRM and DOM models can serve as a solution for a swift investigation of the radiative heat transfer in participating media of real industrial furnaces.

References

[1] Ren, T., Modest, M. F., Fateev, A., Sutton, G., Zhao, W., Rusu, F. Machine learning applied to retrieval of temperature and concentration distributions from infrared emission measurements, (2019) Applied Energy, 252, pp. 113448.

[2] Modest, M. F., Haworth, D. C. Radiative heat transfer in high-pressure combustion systems, (2016) In SpringerBriefs in Applied Sciences and Technology (pp. 137–148). Springer Verlag.

[3] Vujanović, M., Wang, Q., Mohsen, M., Duić, N., Yan, J. Sustainable energy technologies and environmental impacts of energy systems, (2019) Applied Energy, 256, pp. 113919.

[4] Maginot, P. G., Ragusa, J. C., Morel, J. E. High-order solution methods for grey discrete ordinates thermal radiative transfer, (2016) Journal of Computational Physics, 327, pp. 719–746.

[5]   Mishra, S. C., Chugh, P., Kumar, P., Mitra, K. Development and comparison of the DTM, the DOM and the FVM formulations for the short-pulse laser transport through a participating medium, (2006) International Journal of Heat and Mass Transfer, 49, pp. 1820–1832.

[6]   Coelho, P. J. Advances in the discrete ordinates and finite volume methods for the solution of radiative heat transfer problems in participating media, (2014) Journal of Quantitative Spectroscopy and Radiative Transfer. Elsevier Ltd.

[7]   Honus, S., Juchelková, D. Mathematical models of combustion, convection and heat transfer in experimental thermic device and verification, (2014) Tehnicki Vjesnik, 21, pp. 115–122.

[8]   Coelho, P. J., Carvalho, M. G. A Conservative Formulation of the Discrete Transfer Method, (1997) Journal of Heat Transfer, 119, pp. 118–128.

[9]   Chai, J. C., Lee, H. S., Patankar, S. V. Finite Volume Method for Radiation Heat Transfer, (1994) Journal of Thermophysics and Heat Transfer, 8, pp. 419–425.

[10]   Coelho, P. J. Advances in the discrete ordinates and finite volume methods for the solution of radiative heat transfer problems in participating media, (2014) Journal of Quantitative Spectroscopy and Radiative Transfer, 145, pp. 121–146.

[11]   Mishra, S. C., Roy, H. K. Solving transient conduction and radiation heat transfer problems using the lattice Boltzmann method and the finite volume method, (2007), Journal of Computational Physics, pp. 89–107.

[12]   Coelho, P. J. Radiative Transfer in Combustion Systems, (2018) In Handbook of Thermal Science and Engineering, Springer International Publishing, pp. 1173–1199.

[13]   Modest, M. F. Radiative Heat Transfer, Elsevier, Amsterdam, The Netherlands, 2013.

[14]   Tulwin, T. A Coupled Numerical Heat Transfer in the Transient Multicycle CFD Aircraft Engine Model, (2016) Procedia Engineering, 157, pp. 255–263.

[15]   Silva, J., Teixeira, J., Teixeira, S., Preziati, S., Cassiano, J. CFD Modeling of Combustion in Biomass Furnace, (2017) Energy Procedia, 120, pp. 665–672.

[16]   Wang, J., Liu, Y., Sundén, B., Yang, R., Baleta, J., Vujanović, M. Analysis of slab heating characteristics in a reheating furnace, (2017) Energy Conversion and Management, 149, pp. 928–936.

[17]   Mikulčić, H., Baleta, J., Klemeš, J. J. Sustainability through combined development of energy, water and environment systems, (2020) Journal of Cleaner Production. Elsevier Ltd.

[18]   Johnson, T. R., Beer, J. M. Radiative heat transfer in furnaces: Further development of the zone method of analysis, (1973) Symposium (International) on Combustion, 14, pp. 639–649.

[19]   Vujanović, M., Baburić, M., Schneider, D., Duić, N., Priesching, P., Tatschl, R. User function approach in modelling of nitrogen oxides in commercial CFD code FIRE, (2005) Proceedings of the ECCOMAS Thematic Conference on Computational Combustion.

[20]   AVL AST GmbH FIRE Documentation v2019, AVL AST GmbH, Graz, Austria, 2019.

[21]   Jurić, F., Petranović, Z., Vujanović, M., Katrašnik, T., Vihar, R., Wang, X., Duić, N. Experimental and numerical investigation of injection timing and rail pressure impact on combustion characteristics of a diesel engine, (2019) Energy Conversion and Management, 185, pp. 730–739.

[22]   Józsa, V., Kun-Balog, A. Stability and emission analysis of crude rapeseed oil combustion, (2017) Fuel Processing Technology, 156, pp. 204–210.

[23]   Baburić, M., Duić, N., Raulot, A., Coelho, P. J. Application of the Conservative Discrete Transfer Radiation Method to a Furnace with Complex Geometry, (2005) Numerical Heat Transfer, Part A: Applications, 48, pp. 297–313.

[24]   Qi, F., Wang, Z., Li, B., He, Z., Baleta, J., Vujanovic, M. Numerical study on characteristics of combustion and pollutant formation in a reheating furnace, (2018) *Thermal Science*, 22, pp. 2103–2112.

[25]   Filkoski, R., Petrovski, I., Karas, P. Optimization of pulverised coal combustion by means of CFD/CTA modeling, (2006) *Thermal Science*, 10, pp. 161–179.

[26]   Honus, S., Pospíšilík, V., Jursová, S., Šmída, Z., Molnár, V., Dovica, M. Verifying the Prediction Result Reliability Using k-ε, Eddy Dissipation, and Discrete Transfer Models Applied on Methane Combustion Using a Prototype Low-Pressure Burner, (2017) Advances in Science and Technology Research Journal, 11, pp. 252–259.

[27]   Csemány, D., Józsa, V. Fuel Evaporation in an Atmospheric Premixed Burner: Sensitivity Analysis and Spray Vaporization, (2017) *Processes*, 5, pp. 80.

[28]   Abraham, J., Magi, V. Application of the Discrete Ordinates Method to Compute Radiant Heat Loss in a Diesel Engine, (1997) Numerical Heat Transfer, Part A: Applications, 31, pp. 597–610.

[29]   Hosseini Sarvari, S. M. Solution of multi-dimensional radiative heat transfer in graded index media using the discrete transfer method, (2017) International Journal of Heat and Mass Transfer, 112, pp. 1098–1112.

[30]   Dorigon, L. J., Duciak, G., Brittes, R., Cassol, F., Galarça, M., França, F. H. R. WSGG correlations based on HITEMP2010 for computation of thermal radiation in non-isothermal, non-homogeneous H_2O/CO_2 mixtures, (2013) International Journal of Heat and Mass Transfer, 64, pp. 863–873.